PHOTONIC SENSORS / Vol. 16, No. 1, 2026: 9560002

Reconfigurable Fiber Random Laser for Computational Super-Resolution Spectroscopy

Mingzhu SHE[1], Hesheng YONG[1], Zhenchuan LIU[1], and Weili ZHANG[1,2*]

[1]*Key Laboratory of Optical Fiber Sensing & Communications (Ministry of Education of the People's Republic of China), University of Electronic Science and Technology of China, Chengdu 611731, China*

[2]*Tianfu Jiangxi Laboratory, Chengdu 641419, China*

[*]Corresponding author: Weili ZHANG E-mail: wl_zhang@uestc.edu.cn

Abstract: High-resolution spectral measurement is essential for revealing the intrinsic material and structural properties, with broad applications in gas detection, environmental monitoring, biosensing, and materials analysis. Conventional strategies for enhancing spectral resolution typically focus on improving spectrometer hardware or employing sophisticated computational techniques, but they often face trade-offs between the resolution and bandwidth, or the high cost and measurement complexity. Super-resolution spectroscopy enabled by random lasers recently emerged as a promising strategy, yet existing implementations suffering from uncontrolled sampling signals and inefficient data acquisition. Here, we propose a reconfigurable fiber random laser that enables computational super-resolution spectroscopy. By integrating a multimode-single mode fiber filtering structure with controllable input wavefront modulation inside the laser, the system generates narrow-linewidth, sparse, and randomized emission modes, enabling flexible and efficient one-path spectroscopy without relying on the extra reference path. Our experiment compares pre-recorded reference modes with selectively reloaded sampling modes to reconstruct high-resolution spectra. Experimental results demonstrate a 2.2-fold enhancement in spectral resolution compared to the baseline spectrometer, which originally had 70 pm resolution. This work offers a versatile and low-cost solution for super-resolution spectroscopy, with the significant potential for a wide range of optical sensing applications.

Keywords: Fiber random laser; super resolution; spectroscopy.

Citation: Mingzhu SHE, Hesheng YONG, Zhenchuan LIU, and Weili ZHANG, "Reconfigurable Fiber Random Laser for Computational Super-Resolution Spectroscopy," *Photonic Sensors*, 2026, 16(1): 9560002.

1. Introduction

Spectroscopic analysis provides an accurate means of revealing intrinsic structural and material properties, and it has found widespread applications in materials analysis, food safety testing, biosensing, environmental monitoring, and gas sensing [1–5]. With the growing demand for high-precision analysis, the acquisition of high-resolution spectra has become a critical requirement. Effective strategies for enhancing spectral resolution generally fall into two categories: 1) direct improvement of spectrometer performance, including resolution, stability, and sampling rate; 2) advancement of spectral sampling and processing methods, such as

Received: 24 September 2025 / Revised: 6 November 2025

DOI: 10.26599/PhoS.2026.9560002
Article type: Research article

redundant sampling, random sampling, Fourier interpolation, deconvolution, and compressed sensing.

Among these, improving the performance of spectrometers remains the most straightforward approach to enhance spectral resolution. Conventional baseline spectrometers typically adopt Czerny-Turner or Rowland-circle configurations, in which gratings are used for dispersion and aberration-correction techniques are applied to improve resolution [6]. However, the dispersive capability of such instruments heavily depends on the grating-detector separation, resulting in generally bulky systems, with an inherent trade-off between the bandwidth and resolution. Cross-dispersion spectrometers, integrating two orthogonal dispersive elements with a two-dimensional charge coupled device (CCD) array, have been developed to overcome the limitations of the traditional mechanical scanning. Nevertheless, their key dispersive components (e.g., virtual image phase arrays [7] or echelle gratings [8]) are expensive, and the intricate optical layouts may introduce aberrations, thereby constraining the precision of spectral reconstruction.

With the advancement of computational science, computational spectroscopy based on prior calibration and reconstruction algorithms gradually emerged. B. Redding *et al*. [9] developed a speckle spectrometer that exploits the mapping between speckle patterns and wavelengths, combined with convex optimization algorithms for spectral inversion, achieving a high-precision measurement of 1 pm at the 1 550 nm band. This approach requires only three components – a calibration light source, a scattering medium, and a camera – making it simple, low-cost, and precise. To achieve the high resolution, large bandwidth, and high stability, researchers have developed various spatial, on-chip, and waveguide-based speckle spectrometers, employing scattering media such as integrating spheres [10], disordered photonic chips [11], conical helical waveguides [12], scattering hole arrays [13], metasurface [14], and fiber waveguides [15, 16]. Experimentally, speckle multiplexing [17] and oversampling [18] have been utilized to further enhance the bandwidth and resolution; while algorithmically, neural network-based reconstruction methods effectively suppress the resolution-limiting effects of spectral decoherence and significantly reduce reconstruction errors [19, 20]. The resolution of such spectrometers depends primarily on the scanning step size of the calibration light source and the spectral decorrelation bandwidth of the scattering medium. While they provide excellent analytical performance for the simple emission spectrum, calibrating the transmission matrix is time-consuming; for complex sample absorption spectra, speckle inversion may fail to converge or produce distorted spectra. It has been proposed that the entire transmission matrix could be inferred from a single pinhole diffraction speckle pattern to save calibration time [21], but discrepancies between simulated diffraction and actual measurements limit the achievable resolution. The well-known dispersive Fourier-transform spectroscopy maps pulse spectra into time-domain intensity signals for detection [22]. To avoid spectral aliasing, it is applicable only to pulsed light sources and is unsuitable for continuous spectra. Moreover, its resolution scales with the amount of group delay dispersion, while higher-order dispersion inevitably introduces spectral distortion. Fourier-transform spectrometers reconstruct spectra by performing the Fourier transform to interferograms [23]. Their resolution is fundamentally limited by the maximum optical path difference, making it challenging to resolve fine absorption lines.

Another strategy for improving the spectral resolution is to refine spectral sampling and processing methods. In recent years, super-resolution spectroscopy techniques emerged, introducing novel sampling mechanisms and optimizing computational procedures that can

surpass the diffraction-limited resolution of optical systems at low cost and minimal complexity, thereby showing the great potential for practical applications [24–29]. Random lasers, owing to their flexible controllability, randomness, and high sampling resolution [30, 31], have been regarded as ideal light sources for super-resolution spectroscopy [32–35]. A typical random-laser-based super-resolution spectroscopy system involves two steps: random spectral sampling followed by super-resolution reconstruction. Despite the notable progress in the resolution enhancement, it still faces two critical challenges: 1) the non-uniform statistical distribution of random-laser emission in the spectral domain leads to the acquisition of redundant signals, thereby reducing measurement efficiency, and 2) the unknown sampling signals necessitate simultaneous acquisition of both the reference and sampled spectra, which restricts the spectrometer design to a fixed architecture combining dispersive gratings with detector arrays [32, 33], limiting flexibility and generality of measurement schemes.

Here, we propose a reconfigurable fiber random laser (R-FRL) that enables computational super-resolution spectroscopy. Specifically, the system employs a filtering structure composed of multimode fibers (MMFs) and single-mode fiber (SMF), where the modulated wavefront is used to generate randomly filtered spectra. When integrated into the laser cavity, this structure produces the narrow-linewidth, sparse, and random emission modes. By mapping input wavefronts to emission modes (reference signals) and selectively reloading a subset of them during measurement (sampled signals), the transmission (reflection) spectrum can be reconstructed by comparing sampled signals with pre-recorded references. This approach enhances the control over random modes and offers several advantages: 1) low cost, high sampling resolution, and flexible bandwidth, 2) rapidly tunable and precisely controlled sampling spectra, effectively reducing redundant signals, and 3) independence from the reference optical path, enabling flexible measurement methods compatible with various spectroscopic instruments. The proposed system achieves sampling resolution better than 20 pm, covering a 20 nm bandwidth in the 1 550 nm range. Through one-path sampling and spectral reconstruction, it delivers a 2.2-fold enhancement over the baseline spectrometer which originally exhibited resolution of 70 pm. The R-FRL based computational super-resolution spectroscopy provides a high-resolution, efficient, and flexible platform for spectral measurements, promising new perspectives and approaches for applications in super-resolution spectral sensing and analysis.

2. Principle and method

Analogous to single-molecule localization techniques in super-resolution imaging [26, 36], the core concept of the super-resolution spectroscopy lies in performing random and redundant sampling of the spectral sample, followed by comparing the reference and sampling signals to reconstruct the high-resolution spectra. Since the sampling signals are sufficiently sparse and random, and exhibit narrow linewidths, fine spectral details are carried by the sampling peaks, which remain distinguishable at the statistical level. Unlike previous methods, the proposed computational super-resolution spectroscopy based on the R-FRL allows the sampling signals to be both controllable and known, thereby reducing the reliance on reference signals during the sampling process. The principle is illustrated in Fig. 1(a): during sampling, predefined random modes are used to probe the sample, and by comparing the signals before and after the sample, its transmission or reflection spectra can be retrieved.

The control of the sampling signals is illustrated in Fig. 1(b). The light stimulated by amplified spontaneous emission is first modulated by random wavefronts and then coupled into a segment of the

MMF. High-speed wavefront modulation can be realized with a digital micromirror device (DMD). Due to strong modal dispersion and intermodal dispersion, the output of the MMF exhibits highly randomized spectral and spatial distributions [30, 37]. By connecting the MMF to a small-core SMF, the transmitted spectrum acquires complex and random profiles. When the transmission state of the MMF-SMF structure is fixed, random variation of the incident spatial wavefront (pattern) induces synchronous random changes in the transmission spectrum, thereby establishing a large mapping between input wavefronts and output spectra. Incorporating this random filtering structure into a laser cavity further compresses the linewidth through mode competition and gain sharing, producing narrow-linewidth and sparse emission modes.

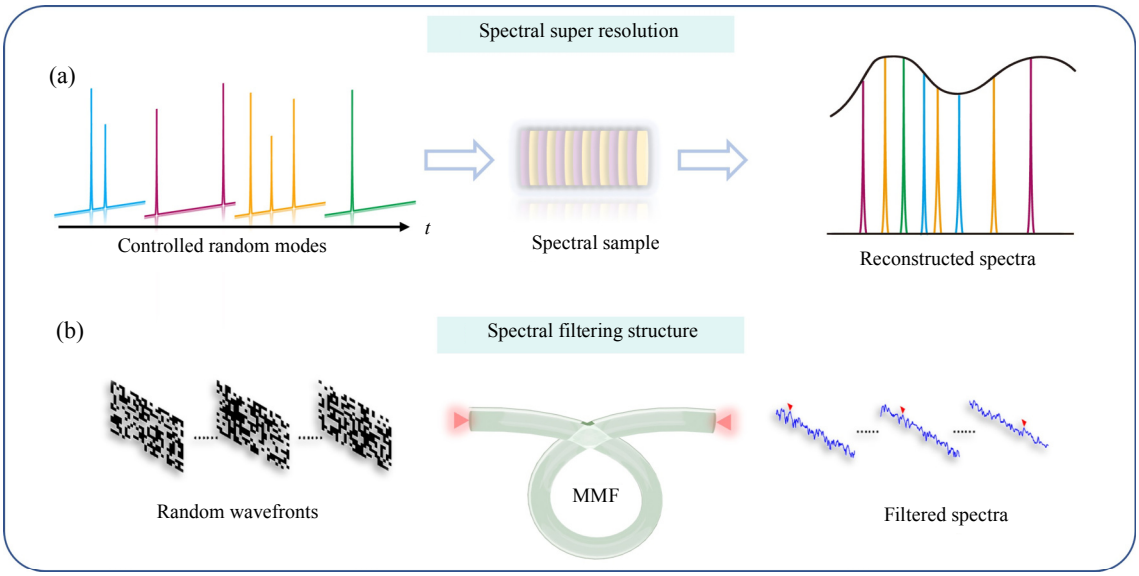

Fig. 1 Principle of the computational super-resolution spectroscopy: (a) principle of computational spectral sampling and reconstruction and (b) method for controlling random sampling modes.

3. Results

3.1 Experimental setup

As shown in Fig. 2, the computational super-resolution spectroscopy system based on the R-FRL consists of two parts: the reconfigurable fiber random laser (Part I) and the computational super-resolution spectroscopy (Part II). In Part I, a 976 nm laser diode pumps a 9.8 m erbium-doped fiber (EDF) to provide the optical gain, while an optical isolator (ISO) ensures unidirectional operation of the intracavity modes. At the cavity end, a lens collimates the beam onto the surface of a DMD, where it undergoes random wavefront modulation. The reflected light is then collected by a ×10 microscope objective and imaged onto the input facet of a 3 m MMF. The MMF output is connected to a standard SMF, together forming a filtering structure. Downstream, a 50:50 coupler directs one port to a wavelength division multiplexer (WDM) to complete a ring-laser cavity, while the other port is reserved for the mode recording and output. In this configuration, random patterns are sequentially loaded onto the DMD to generate reference spectra.

In Part II, a computational super-resolution spectroscopy system is implemented. A Fabry-Perot (F-P) cavity serves as the sample to conceptually demonstrate our computational super-resolution spectroscopy. The R-FRL is coupled to the F-P cavity via an optical circulator for random sampling, and the reflected signal is collected by an optical spectrum analyzer (OSA) with resolution of 70 pm.

Random patterns, related to predefined spectra, i.e., the reference spectra, are selectively reloaded onto the DMD again to acquire the sampled reflection spectra of the F-P cavity. Those recurring spectra will not be reloaded to enhance the sampling efficiency. The wavelength positions of the reference and sampled spectra are then localized, and the reflection spectrum of the F-P cavity is retrieved by comparing their respective intensity values.

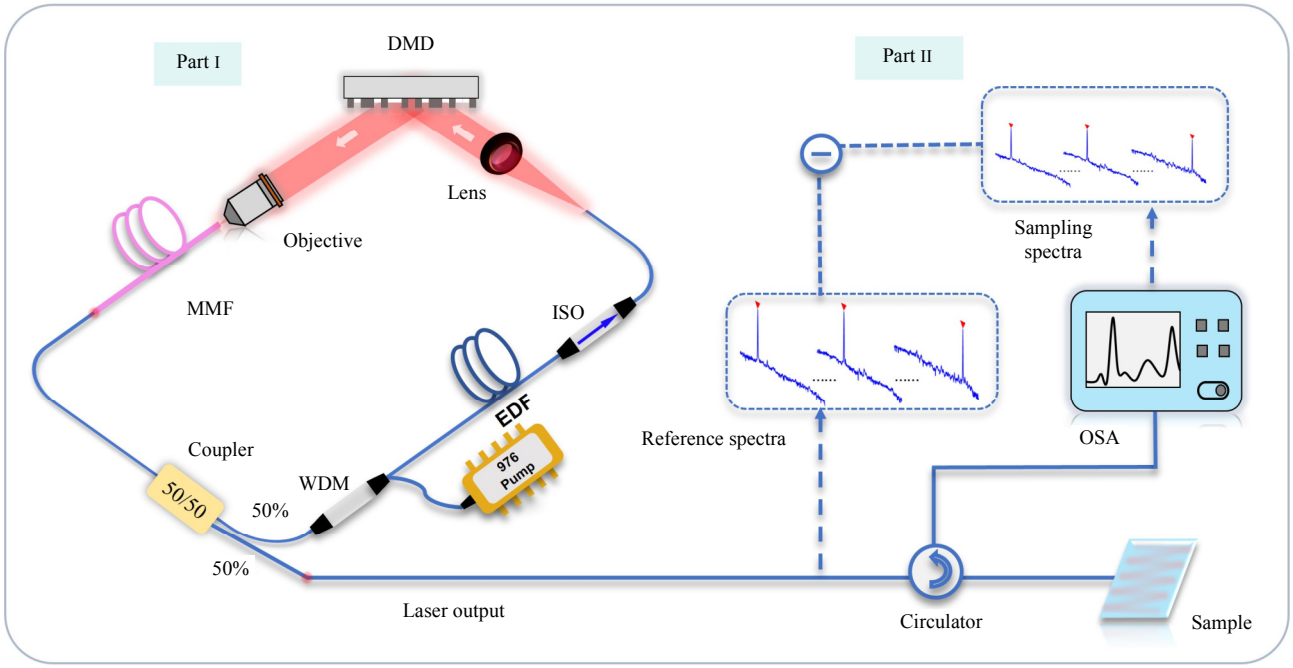

Fig. 2 Setup of the R-FRL and computational super-resolution spectroscopy. The minus sign indicates that the sampling spectrum is compared with the reference spectrum in dBm units.

3.2 Characteristics of the reconfigurable fiber random laser

The performance of the super-resolution spectroscopy is determined by the characteristics of the R-FRL, specifically its spectral- and time-domain properties. We first analyze the spectral-domain properties statistically, as shown in Fig. 3. Figure 3(a) shows that the laser threshold is approximately 43 mW, with a conversion efficiency of around 2.7%. The statistics of the linewidth are presented in Fig. 3(b), showing an average 6 dB bandwidth of 11.8 pm, with nearly all linewidths below 20 pm, indicating the sampling resolution better than 20 pm. Notably, the linewidth here refers to the envelope width of several adjacent narrow modes. The linewidth is highly dependent on the geometrical properties of the MMF. Both too short and too long optical fiber configurations will deteriorate the filter linewidth. In our setup, a 1 m large-core MMF (105 μm core diameter) is combined with a 2 m small-core MMF (40 μm core diameter) and coiled together. Higher-order modes are fully excited in the large-core MMF and subsequently experience strong dispersion in the small-core MMF, without complete mode homogenization, ultimately yielding narrow-linewidth and sparse mode emissions. Figure 3(c) shows the statistical distribution of laser peak wavelengths, i.e., the emission bandwidth, spanning 1 540 nm–1 560 nm, which is determined by the active gain fiber configuration. Figures 3(d)–3(f) display typical scanning single-, dual-, and triple-peak laser modes within the emission bandwidth. These results demonstrate that

the R-FRL exhibits narrow linewidth, sparsity and randomly distributed yet ergodic wavelengths, satisfying the sampling signal requirements for the super-resolution spectroscopy.

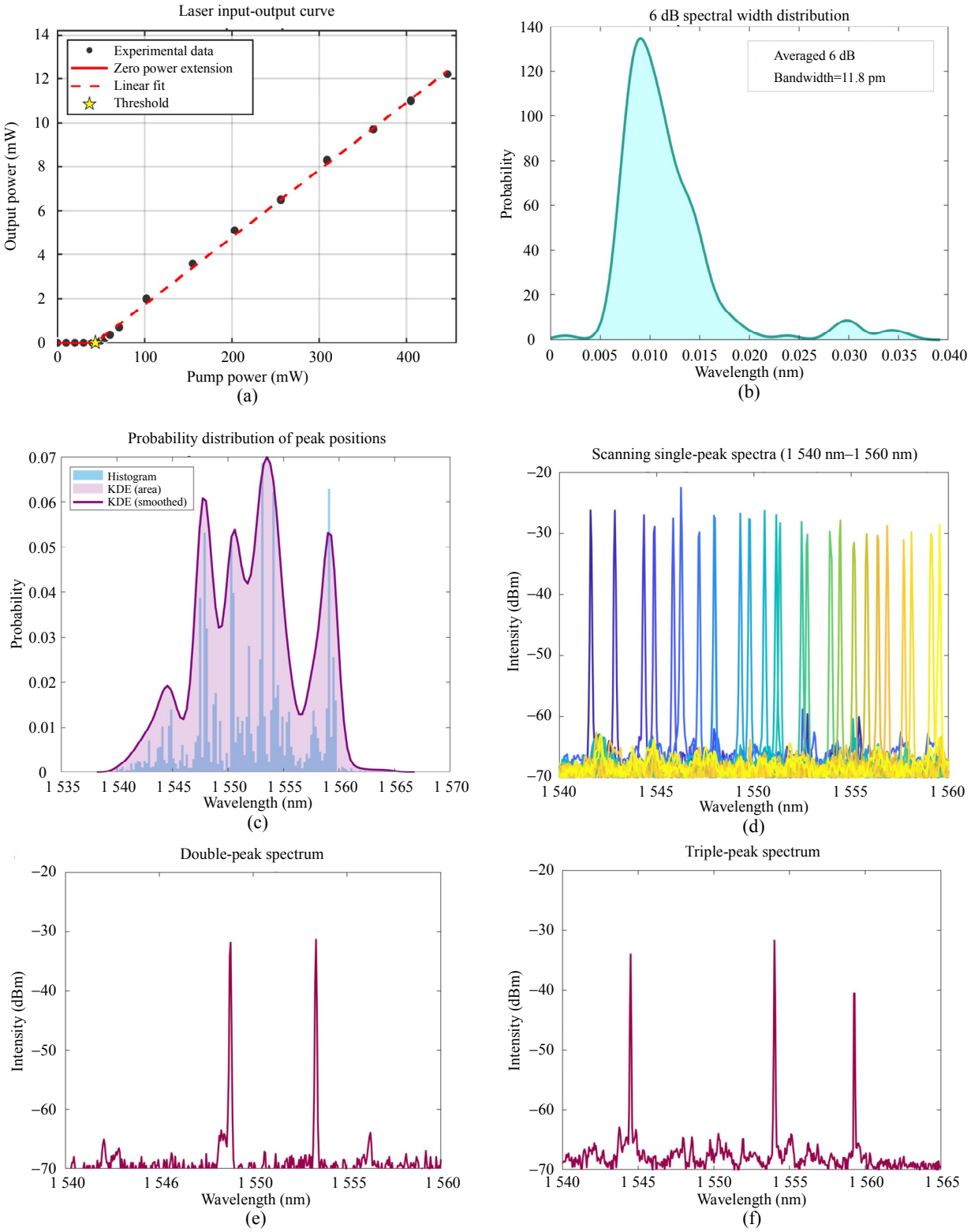

Fig. 3 Spectral characteristics of the R-FRL: (a) laser input-output curve, (b) statistical distribution of laser linewidths, (c) statistical distribution of peak wavelengths, (d) output spectrum of the scanned laser, (e) double-peak laser spectrum, and (f) triple-peak laser spectrum.

The time-domain dynamics of the R-FRL are presented in Fig. 4. The laser build-up time is approximately 2 μs [from Point A to Point B, see Fig. 4(a)], which is much faster than the DMD frame rate. In our experiment, the spectral switching time is 17 ms [from Point C to Point D, see Fig. 4(b)], consistent with the DMD frame rate of 60 Hz. Commercially available DMDs now support higher pattern switching speeds up to several tens of kHz, which can improve the spectral switching time remarkably. The time-domain stability of the R-FRL is illustrated in Figs. 4(c)–4(d), where both the spectrum and its intensity remain stable for over 300 min. These time-domain characteristics demonstrate that the R-FRL exhibits fast switching and temporal stability, thereby enabling high sampling efficiency and reconfigurability.

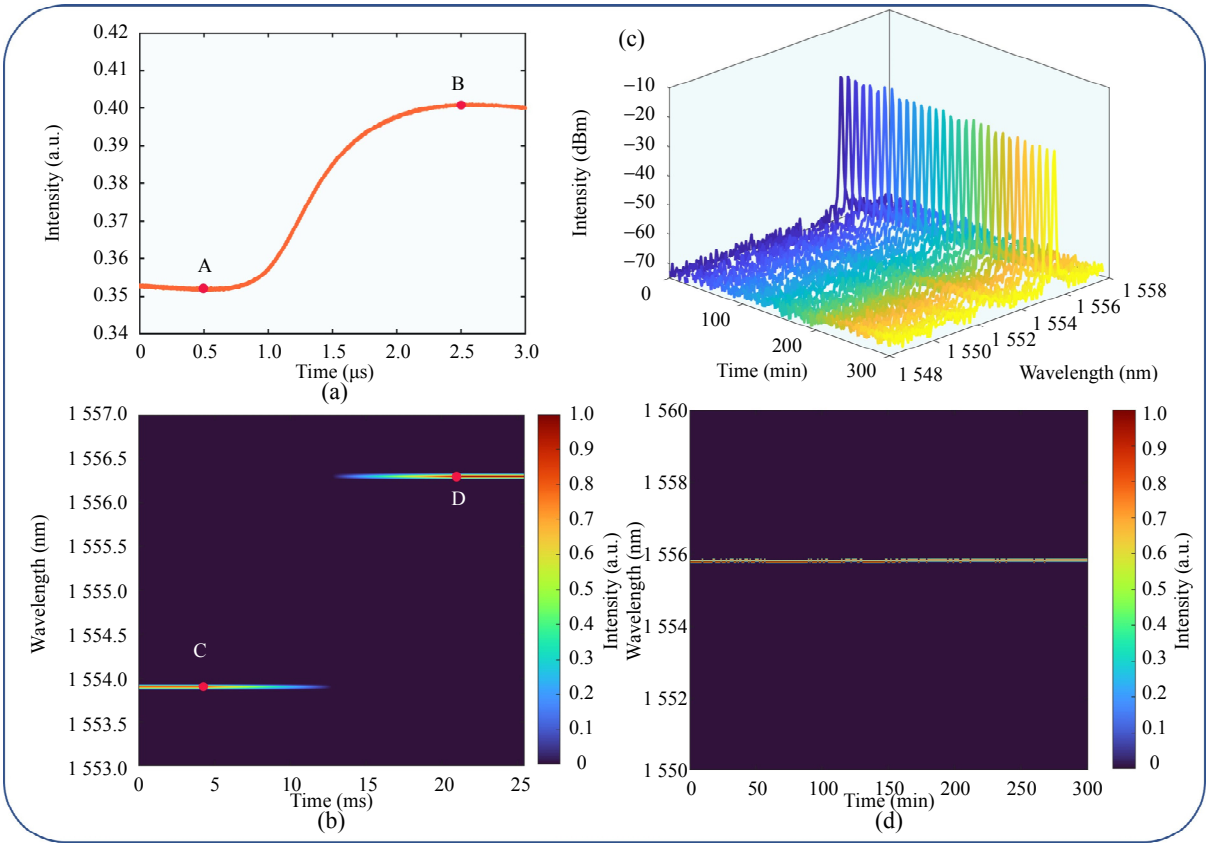

Fig. 4 Time-domain dynamics of the R-FRL: (a) laser build-up time, (b) spectral switching time, (c) and (d) temporal steady-state behaviors of the laser.

3.3 Computational super-resolution spectroscopy

The proposed R-FRL light source integrates both the random sampling and reconfigurability. Here, we demonstrate a proof-of-concept application: computational super-resolution spectroscopy. The setup is shown in Part II of Fig. 2, where an additional bandpass filter (1 549.6 nm–1 550.3 nm) is inserted into the laser cavity in Part I of Fig. 2 to constrain the sampling bandwidth. The tested F-P sample has a free spectral range (FSR) of 31.4 pm. The baseline OSA has the resolution of 70 pm, corresponding to the 2.2 FSR.

Typical measurement results are presented in Fig. 5, where the cyan curves represent the pre-recorded reference spectra, and the magenta curves represent the sampled spectra reflected by the F-P sample. After localizing the reference and sampled spectra, the peak wavelengths are identified, and the reflection spectrum is reconstructed

according to the expression (unit: dBm):

$$T(\lambda) = S(\lambda)_{\text{sam}} - S(\lambda)_{\text{ref}} \quad (1)$$

where the $S(\lambda)_{\text{sam}}$ represents the sampled spectrum and the $S(\lambda)_{\text{ref}}$ represents the reference spectrum at the wavelength λ.

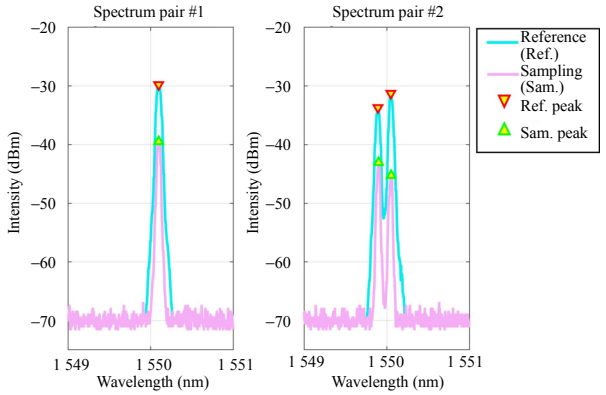

Fig. 5 Reference spectra, sampling spectra, and localizing the peak wavelengths.

The super-resolution reconstruction results are shown in Fig. 6. In Fig. 6(a), the red curve represents the ground-truth of the F-P reflection spectrum with an FSR of 31.4 pm, while the magenta solid line corresponds to the direct measurement using an amplified spontaneous emission source (ASE) with the low-resolution baseline spectrometer (70 pm resolution), where the spectral features are barely discernible. After performing random high-resolution sampling with the proposed R-FRL, the reconstructed reflection spectrum is shown as the blue curve in Fig. 6(b), closely matching the ground truth and achieving the high resolution of 31.4 pm. Figure 6(c) presents the Fourier transforms of the ground truth (red dashed line), the super-resolution reconstructed spectrum (blue solid line), and the low-resolution measurement (magenta solid line), clearly demonstrating that our method significantly enhances spectral resolution by a factor of 2.2, improving it from 70 pm to 31.4 pm. The ultimate resolution of this method is determined by the sampling resolution of the R-FRL, which is better than 20 pm in our case.

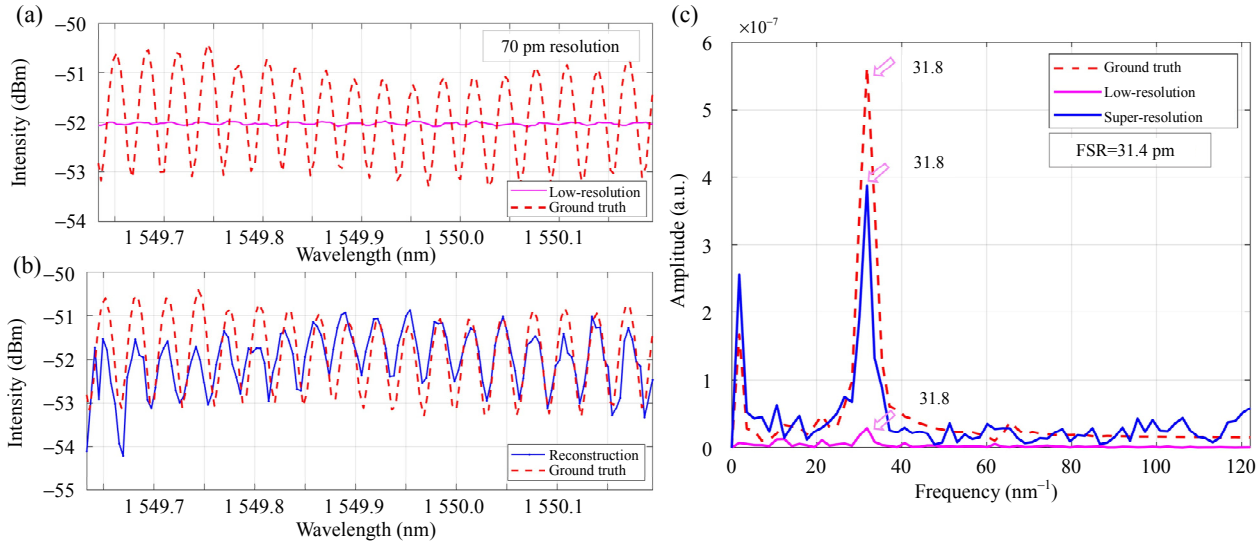

Fig. 6 Super-resolution reconstruction results: (a) ground-truth spectrum of the F-P cavity (red dashed line) and direct measurement using a baseline spectrometer (magenta solid line), (b) ground-truth reflection spectrum of the F-P cavity (red dashed line) and the super-resolution reconstructed spectrum (blue solid line), and (c) fast Fourier transforms of the F-P reflection spectra: ground-truth spectrum (red dashed line), low-resolution measurement (magenta solid line), and super-resolution reconstruction (blue solid line).

4. Conclusions

In conclusion, we have proposed an R-FRL and a corresponding computational super-resolution spectroscopy method. By leveraging random wavefront modulation and an MMF-SMF filtering structure, the realized R-FRL exhibits the narrow linewidth (average ~11.8 pm), sparse peaks (1 peak–3 peaks per emission), and good ergodicity (covering 1 540 nm–1 560 nm). In the

demonstration measurement of the F-P cavity's reflection spectrum, the one-path computational super-resolution spectroscopy enables an improvement of the system resolution from 70 pm to 31.4 pm, corresponding to a 2.2-fold enhancement. Moreover, the R-FRL for spectral sampling is inherently reconfigurable and capable of high-speed operation, potentially boosting both the resolution and measurement efficiency. Overall, the proposed computational super-resolution spectroscopy approach offers a low-cost, flexible, efficient, and high-resolution solution for spectral measurement in applications such as environmental monitoring, food safety, agriculture, and industry. The developed R-FRL architecture further advances the controllability of random lasers, providing new light source solutions and regulatory strategies for super-resolution imaging, spectroscopy, information encryption, and sensing.

Acknowledgment

This work was supported by the National Natural Science Foundation of China (Grant No. 62375040); Innovation Program for Quantum Science and Technology, China (Grant No. 2024ZD0300800); the Exchange Project for Key Lab of Optical Fiber Sensing and Communications (Ministry of Education of China) (Grant No. ZYGX2025K010).

Declarations

Conflict of Interest The authors declare that they have no competing interests.

Permissions All the included figures, tables, or text passages that have already been published elsewhere have obtained the permission from the copyright owner(s) for both the print and online format.

Use of AI Statement None.

References

[1] C. Li, D. Liu, B. Liu, X. Ren, J. Liu, Z. He, *et al.*, "Chang'E-4 initial spectroscopic identification of lunar far-side mantle-derived materials," *Nature,* 2019, 569(7756): 378–382.

[2] K. Wang, Z. Li, J. Li, and H. Lin, "Raman spectroscopic techniques for nondestructive analysis of agri-foods: a state-of-the-art review," *Trends in Food Science & Technology*, 2021, 118: 490–504.

[3] J. Tang, Z. Li, M. Xie, Y. Luo, J. Yu, G. Chen, *et al.*, "Liquid crystal based label-free optical sensors for biochemical application," *Photonic Sensors*, 2024, 14(2): 240203.

[4] Z. Shen, H. D'Agui, L. Walden, M. Zhang, T. M. Yiu, K. Dixon, *et al.*, "Miniaturised visible and near-infrared spectrometers for assessing soil health indicators in mine site rehabilitation," *Soil*, 2022, 8(2): 467–486.

[5] Q. Nie, Z. Liu, M. Cheng, S. Pei, D. Yang, D. Guo, *et al.*, "Review on hollow-core fiber based multi-gas sensing using Raman spectroscopy," *Photonic Sensors*, 2024, 14(4): 240412.

[6] K. S. Lee, K. P. Thompson, and J. P. Rolland, "Broadband astigmatism-corrected czerny-turner spectrometer," *Optics Express*, 2010, 18(22): 23378.

[7] H. Zhou, W. Zhao, B. Fang, B. Lv, W. Cui, W. Zhang, and W. Chen, "A broadband picometer resolution visible CCD spectrometer based on virtually imaged phased array technology," *Analyst*, 2023, 148(18): 4421–4428.

[8] L. Yin, Bayanheshig, J. Yang, Y. Lu, R. Zhang, C. Sun, *et al.*, "High-accuracy spectral reduction algorithm for the échelle spectrometer," *Applied Optics*, 2016, 55(13): 3574.

[9] B. Redding, S. M. Popoff, and H. Cao, "All-fiber spectrometer based on speckle pattern reconstruction," *Optics Express*, 2013, 21(5): 6584–6600.

[10] J. Liang, J. Li, J. He, Y. Guo, X. Ma, Y. Zhang, *et al.*, "Multi-wavelength spectral reconstruction with localized speckle pattern," *Optics Communications*, 2025, 575: 131266.

[11] W. Hartmann, P. Varytis, H. Gehring, N. Walter, F. Beutel, K. Busch, *et al.*, "Waveguide-integrated broadband spectrometer based on tailored disorder," *Advanced Optical Materials*, 2020, 8(6): 1901602.

[12] F. Meng, Y. Zhao, H. Wang, and Y. Zhang, "High-performance compact spectrometer based on multimode interference in a tapered spiral-shaped waveguide," *Optics Express*, 2019, 27(26): 38349.

[13] T. Yang, C. Xu, H. P. Ho, Y. Y. Zhu, X. H. Hong, Q. J. Wang, *et al.*, "Miniature spectrometer based on diffraction in a dispersive hole array," *Optics Letters*, 2015, 40(13): 3217.

[14] J. E. Fröch, S. Colburn, A. Zhan, Z. Han, Z. Fang, A. Saxena, *et al.*, "Dual band computational infrared spectroscopy via large aperture meta-optics," *ACS Photonics*, 2022: acsphotonics.2c01017.

[15] J. Liang, J. Li, Z. Huang, J. He, Y. Guo, X. Ma, *et al.*, "High-resolution miniaturized speckle spectrometry using fuse-induced fiber microvoids," *Photonics Research*, 2025, 13(9): 2654–2667.

[16] Z. Huang, J. Liang, J. Ye, J. He, X. Ma, Y. Zhang, *et al.*, "High-resolution, broadband reconstructive spectrometer enabled by cascaded dispersion," *Optics Express*, 2025, 33(4): 8055–8064.

[17] S. F. Liew, B. Redding, M. A. Choma, H. D. Tagare, and H. Cao, "Broadband multimode fiber spectrometer," *Optics Letteers*, 2016, 41(9): 2029–2032.

[18] Z. Zhang, S. Xiao, Q. Song, and K. Xu, "Scalable on-chip diffractive speckle spectrometer with high spectral channel density," *Light: Science & Applications*, 2025, 14(1): 130.

[19] Y. Xu, J. Wu, H. Li, R. Cai, Y. Zhu, Y. Li, *et al.*, "Compact speckle spectrometer using femtosecond laser-induced double-sided surface nanostructures," *Optics Letters*, 2024, 49(21): 6281.

[20] Y. Wan, X. Fan, B. Xu, and Z. He, "Reconstructive spectrum analyzer with high-resolution and large-bandwidth using physical-model and data-driven model combined neural network," *Laser & Photonics Reviews*, 2023, 17(7): 2201018.

[21] C. Chen, H. Gu, and S. Liu, "Ultra-simplified diffraction-based computational spectrometer," *Light: Science & Applications*, 2024, 13(1): 9.

[22] K. Goda and B. Jalali, "Dispersive fourier transformation for fast continuous single-shot measurements," *Nature Photonics*, 2013, 7(2): 102–112.

[23] A. Herrero-Bermello, J. Li, M. Khazaei, Y. Grinberg, A. V. Velasco, M. Vachon, *et al.*, "On-chip fourier-transform spectrometers and machine learning: a new route to smart photonic sensors," *Optics Letters*, 2019, 44(23): 5840–5843.

[24] L. Santamaria, F. Sgobba, D. Pallotti, and C. Lupo, "Single-photon super-resolved spectroscopy from spatial-mode demultiplexing," *Photonics Research*, 2025, 13(4): 865–874.

[25] D. Malka, G. Berkovic, Y. Hammer, and Z. Zalevsky, "Super-resolved Raman spectroscopy," *Spectroscopy Letters*, 2013, 46(4): 307–313.

[26] W. E. Moerner, "Nobel lecture: single-molecule spectroscopy, imaging, and photocontrol: foundations for super-resolution microscopy," *Reviews of Modern Physics*, 2015, 87(4).

[27] B. Dong, L. Almassalha, B. E. Urban, T. Quyen, S. Khuon, T. L. Chew, *et al.*, "Super-resolution spectroscopic microscopy via photon localization," *Nature Communications*, 2016, 7: 12290.

[28] P. Hu, L. Zhao, and H. Liu, "Infrared spectral super-resolution model with linear canonical transforms regularization for spectral signals," *Infrared Physics & Technology*, 2023, 133: 104850.

[29] L. Chen, P. Yang, B. Xie, and S. Feng, "Super-resolution spectroscopy via spectrum slicing with a Fabry-Perot cavity," *Journal of the Optical Society of America B–Optical Physics*, 2024, 41(4): 1069–1075.

[30] Y. Zhang, S. Wang, M. She, Y. Rao, and W. Zhang, "Spectrally programmable Raman fiber laser with adaptive wavefront shaping," *Photonics Research*, 2023, 11(1): 20.

[31] S. Li, J. Xu, J. Liang, J. Ye, Y. Zhang, X. Ma, *et al.*, "Multi-wavelength random fiber laser with a spectral-flexible characteristic," *Photonics Research*, 2023, 11(2): 159–164.

[32] A. Boschetti, A. Taschin, P. Bartolini, A. K. Tiwari, L. Pattelli, R. Torre, *et al.*, "Spectral super-resolution spectroscopy using a random laser," *Nature Photonics*, 2020, 14(3): 177–182.

[33] Y. Zhang, S. Wang, C. Zheng, and W. Zhang, "Coherent random fiber laser-enabled super-resolution spectroscopy," *ACS Photonics*, 2023, 10(8): 2670–2678.

[34] Z. Liu, M. She, J. Wen, Y. Rao, and W. Zhang, "Sparking fiber random laser for wavelength scanning," *Proceedings of SPIE*, 2025, 13639: 136396B.

[35] Z. Wang, S. Wang, R. Ma, Y. Liu, H. Zhu, Y. Zhang, *et al.*, "Near-infrared speckle-illumination imaging based on a multidimensionally disordered fiber laser," *Physical Review Applied*, 2022, 18(2): 024031.

[36] W. Zhao, S. Zhao, Z. Han, X. Ding, G. Hu, L. Qu, *et al.*, "Enhanced detection of fluorescence fluctuations for high-throughput super-resolution imaging," *Nature Photonics*, 2023, 17(9): 806–813.

[37] M. She, Z. Wang, Y. Zhang, A. Shi, and W. Zhang, "Spectral shaping enabled mode control and information transmission through a multimode optical fiber," *IEEE Photonics Technology Letters*, 2024, 36(5): 357–360.